



# UNIVERSITÀ DI PARMA

## ARCHIVIO DELLA RICERCA

University of Parma Research Repository

Alginate/human elastin-like polypeptide composite films with antioxidant properties for potential wound healing application.

This is the peer reviewed version of the following article:

*Original*

Alginate/human elastin-like polypeptide composite films with antioxidant properties for potential wound healing application / Bergonzi, Carlo; Gomez D'Ayala, Giovanna; Laurienzo, Paola; Bandiera, Antonella; Catanzano, Ovidio; Elviri, Lisa. - In: INTERNATIONAL JOURNAL OF BIOLOGICAL MACROMOLECULES. - ISSN 0141-8130. - 164:(2020), pp. 586-596. [10.1016/j.ijbiomac.2020.07.084]

*Availability:*

This version is available at: 11381/2880121 since: 2020-09-14T12:35:00Z

*Publisher:*

Elsevier B.V.

*Published*

DOI:10.1016/j.ijbiomac.2020.07.084

*Terms of use:*

Anyone can freely access the full text of works made available as "Open Access". Works made available

*Publisher copyright*

note finali coverpage

(Article begins on next page)

02 May 2026

# Alginate/human elastin-like polypeptide composite films with antioxidant properties for potential wound healing application

Carlo Bergonzi <sup>a,1</sup>, Giovanna Gomez d'Ayala <sup>b,1</sup>, Lisa Elviri <sup>a</sup>, Paola Laurienzo <sup>b</sup>, Antonella Bandiera <sup>c</sup>, Ovidio Catanzano <sup>c,\*</sup>

<sup>a</sup> Food and Drug Department, University of Parma, Parco Area delle Scienze 27/A, 43124 Parma, Italy

<sup>b</sup> Institute for Polymers, Composites and Biomaterials (IPCB) – CNR, Via Campi Flegrei 34, 80078 Pozzuoli (NA), Italy

<sup>c</sup> Department of Life Sciences, University of Trieste, Via Licio Giorgieri 1, 34127 Trieste, Italy

## ARTICLE INFO

### Article history:

Received 1 April 2020

Received in revised form 18 June 2020

Accepted 9 July 2020

Available online 15 July 2020

### Keywords:

Alginate

Human Elastin-Like Polypeptide

Structural and thermal characterization

Composite film

Drug delivery

Biomimetic material

## ABSTRACT

In this contribution we describe the preparation and characterization of a series of cross-linked films based on the combination of an elastin-derived biomimetic polypeptide (Human Elastin-Like Polypeptide, HELP) with alginate (ALG) to obtain a composite with enhanced properties. ALG/HELP composite films loaded with the hydrophobic natural antioxidant curcumin were prepared by solvent casting method followed by the cross-linking with calcium chloride. The compatibility between the two components as well as the final properties was evaluated. The micro-morphological study of films showed a homogeneous structure, but the film tensile strength decrease with HELP content and elongation at break was adversely affected by biopolymer addition. Spectroscopic and thermal analyses confirmed an interaction between ALG and HELP which also causes a modification in swelling kinetics and faster degradation. Moreover, the study of curcumin release showed a controlled delivery up to 10 days with a faster release rate in the presence of HELP. Human Dermal Fibroblasts (hDF) were used to test the *in vitro* cytocompatibility. The antioxidant activity correlated to the increase of HELP content suggested the applicability of these composites to develop smart biomaterials. Overall, these features indicated how this composite material has considerable potential as customizable platforms for various biomedical applications.

## 1. Introduction

Natural polymers derived from microbial, plant, or animal sources have been extensively investigated for applications in regenerative medicine as they possess some structural similarities with the natural supporting structures of the body, such as connective tissues and extracellular matrix (ECM). They are non-toxic, biocompatible and particularly versatile and adaptable to technological needs, due to the presence of different functional groups in their structure. A large number of studies have been carried out to investigate the potential applications of natural polymers in regenerative medicine, exploring the relationship between the polymer nature, its physical form (such as hydrogels, microspheres, microcapsules, sponges, foams, and fibers) [1,2]. An efficient way to tune the biopolymer-based biomaterial properties, towards a wide range of biomedical applications, is their combination with other components (organic or inorganic) to prepare a new range of composites with unique properties. This approach allows the

development of materials with specific features in terms of biodegradability, mechanical strength, gelation property and cell compatibility, possessing properties that are different from those of the original components. Moreover, composite materials allow a flexible design, since their structure and properties can be optimized and tailored to specific applications [3].

Alginate (ALG) represents a whole family of linear copolymers composed of both (1,4)-linked  $\beta$ -D-mannuronate (M) and  $\alpha$ -L-guluronate (G) residues in different proportions, mainly depending on the source. Physical properties and molecular weight of ALG strictly depend on the sequence of M and G units, as well as the cross-linking which occurs by the co-operative binding of divalent cations and the G-block regions of the copolymer. To take advantage of the biocompatibility and biodegradability under physiological conditions, ALG is often used in combination with other materials, such as synthetic and natural polymers (Poly Lactic-co-Glycolic Acid (PLGA), Polyethylene Glycol (PEG), and chitosan), proteins (collagen and gelatin), ceramic materials, and bioactive glass to prepare new supports for tissue engineering [4–7]. Each of the reported composite material has its peculiar properties, however, the combination between ALG and proteins represents a promising strategy to enhance the cellular interaction of alginate and to tailor the biodegradability of the final materials for tissue regeneration [8].

\* Corresponding author at: Department of Pharmacy, University of Naples Federico II, Via D. Montesano 49, 80131 Naples, Italy.

E-mail address: ovidio.catanzano@unina.it (O. Catanzano).

<sup>1</sup>These authors contributed equally to the work.

Elastin is one of the most abundant proteins in the native ECM [9]. The high content of hydrophobic amino acids makes elastin one of the most chemically resistant and durable proteins in the entire body [9]. In nature, elastin has a fundamental role in the extracellular matrix as it confers rubber-like elasticity to the tissues, allowing them to sustain indefinite cycles of deformation/relaxation without rupture [10]. For this reason, elastin represents an attractive component for composite fabrication as it may provide elastic recoil to stiffer materials. Moreover, elastin interacts with cells *via* a large number of cell surface receptors, enhancing skin fibroblast, vascular smooth muscle cells and endothelial cells proliferation [11,12] and having a biological effect on acceleration and enhancement of skin wound repair [13]. Unfortunately, the hydrophobic nature of elastin and its extensive cross-linked structure makes it difficult to be processed into biomaterials [14]. Hence, soluble and recombinant forms of elastin such as tropoelastin, alpha-elastin, and synthetic elastin-like polypeptides (ELPs) have been used to prepare composites scaffolds [15].

Human Elastin-Like Polypeptides (HELPS) are a class of bio-inspired polypeptides developed as an alternative to the elastin of animal origin. HELPS are artificial, genetically encodable biopolymers based on the hexapeptidic VAPGVG repeated motif [16] that have proven to be excellent components for drug delivery and tissue engineering applications due to their good cyto- and bio-compatibility, their ease of handling, design, production, and modification [17]. Furthermore, thanks to the presence of glutamine and lysine residues in their primary structure, HELP can be cross-linked under the action of transglutaminase (TG) to form stable hydrogels without the use of harsh chemicals like glutaraldehyde or analogous cross-linking agents [18]. In previous works, we have synthesized and tested a series of HELPS with different structures and properties as adhesion substrates for muscle cells [19,20], model systems for elastolytic activity detection [21], and drug delivery devices [17,22]. However, the potential of HELPS as a component of composite biomaterials has not been fully explored yet.

Recently, a composite material based on the deposition of HELP on electrospun poly-L-lactic acid fibers (PLLA-HELP) was developed by our group demonstrating the suitability of this protein to prepare readily customizable biomaterials with specific functionality [23]. Here, we decided to assess the combination of HELP with a natural polymer (ALG) to obtain a composite with enhanced chemical-physical properties. Therefore, the aim of this work was to investigate the interactions between the two components and to evaluate the potential of the obtained composite to realize customizable platforms for drug delivery of multifunctional agents. A series of ALG-based polymeric films with different concentration of HELP were prepared and loaded with the model compound curcumin. As far as we know, this is the first study reporting the preparation of a biomaterial based on ALG and HELP for the delivery of a natural product.

## 2. Experimental

### 2.1. Materials

Sodium alginate (Ph.Eur. grade, MW 180–300 kDa, Lot. 9C260/DOC) was purchased from Carlo Erba reagents (Milano, Italy). Yeast extract, tryptone, NaCl and antibiotics for *E. coli* growth were from Duchefa Biochemie. For cell culture, Dulbecco's modified eagle medium (DMEM) was purchased from Lonza Group (Basel, Switzerland), fetal bovine serum (FBS), penicillin/streptomycin solution and trypsin/EDTA solution were from Aurogene (Rome, Italy), and Resazurin sodium salt was from Alfa Aesar (Ward Hill, MA, USA). Curcumin, 2, 2-diphenyl-1-picrylhydrazyl (DPPH) and all the other products and chemicals used during the experiments were obtained from Sigma Aldrich (St. Louis, USA) and were of reagent grade with the highest purity available. Deionized ultra-filtered water was used throughout this study.

### 2.2. Production of HELP polypeptide

HELP recombinant biopolymer was prepared as previously reported [21]. The recombinant product was expressed in a C3037 *E. coli* strain (New England Biolabs, Ipswich, MA) and then subjected to an extraction and purification procedure exploiting its inverse phase transition properties. Briefly, the pellet obtained from 1.2 l of IPTG-induced bacterial culture was re-suspended in 400 ml of extraction buffer (50 mM Tris/HCl pH = 8, 250 mM NaCl, 0,1 mM EDTA, 0,1% Triton X-100, 1 mM PMSF) and disrupted using a high-pressure homogenizer (Panda NS1001L, GEA Niro Soavi, Germany). To eliminate the solid bacterial residues, the recovered suspension was added with 20 mM 2-mercaptoethanol, cooled on ice, and finally centrifuged at 10000 rpm, for 30 min at 8 °C (Beckman–Coulter, J-26 XP). The separation of the recombinant biopolymers of interest from the supernatant was obtained using a series of temperature-dependent transition cycles. Aggregated HELP polypeptide particles were obtained adding NaCl to a final concentration of 0.5 M at 37 °C and separated by centrifugation at 10000 rpm, 37 °C for 30 min. The pellet was re-dissolved in cold water and all the non-soluble material was discarded by cold centrifugation (10,000 rpm, 8 °C for 10 min). The temperature of the resulting solution was raised to 37 °C and the protein was precipitated again by NaCl addition. Three of these cycles were sufficient to obtain the pure recombinant protein. The polypeptide was frozen overnight at –80 °C, and then lyophilized at 0.01 atm and –60 °C in a Modulyo apparatus (Edwards, Crawley, UK) for long-term storage. The HELP recombinant polypeptide obtained was analyzed by sodium dodecyl sulfate – polyacrylamide gel electrophoresis (SDS-PAGE).

### 2.3. Preparation of alginate/HELP composite film

The ALG/HELP composite films were prepared by solvent casting method. The entire preparation procedure is summarized in Fig. 1. Alginate (1% w/v) was dissolved in ultrapure water together with HELP at two different concentrations (0.125 and 0.25% w/v) and glycerol (2:1 w/w alginate/glycerol). The mixture was kept under magnetic stirring at 4 °C, for at least 6 h. A solution of curcumin in acetone (20 mg/ml) was added to the resultant ALG/HELP gel to obtain a final concentration of 0,1% w/v. The curcumin-loaded ALG/HELP gel was gently mixed under magnetic stirring, at 4 °C for 30 min. 4 ml of this dispersion was then poured into Petri dishes with a diameter of 35 mm and left overnight in an oven at 37 °C, to favor solvent evaporation. Three different films, named ALCur 1 (no HELP) HALCur 1 (0.125% w/v HELP) and HALCur 2 (0.25% w/v HELP) all loaded with the same amount of curcumin were prepared to test the effect of the presence of HELP on the properties of the composites. Moreover, an ALG alone film without curcumin (Ca-ALG) was prepared as described above as control for FT-IR and thermal analysis. All the dried films were crosslinked by immersion in a solution of calcium chloride 5% (w/v) for 15 min. After crosslinking, the samples were washed with abundant ultrapure water several times and further dried in the oven to obtain the final films. After preparation, all the films were visually examined to identify any physical defects.

### 2.4. Scanning electron microscopy (SEM)

The morphology of film surfaces was evaluated, by using a scanning electron microscope (Philips 501, Holland). Films were freeze-dried for 24 h with an Alpha 2–4 LCS Plus freeze dryer (Martin Christ, Osterode am Harz, Germany) and the anhydrous hydrogels were then coated with gold (thickness 60 nm).

### 2.5. Mechanical characterization

Mechanical properties of ALCur, HALCur 1 and HALCur 2 were evaluated by using a traction dynamometer (Acquati AG MC1, Italy). Before

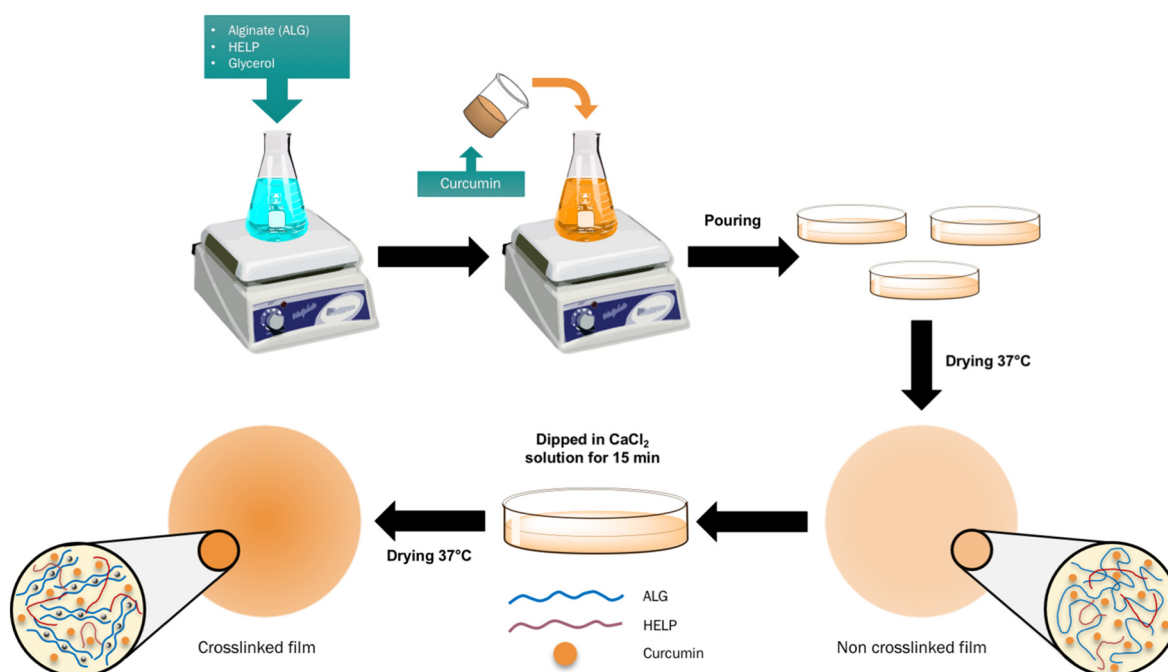


Fig. 1. Scheme of ALG/HELP composite film preparation.

the traction test, the films were accurately cut in rectangles with a predetermined size of 25 × 16 mm. Each sample was tested in triplicate. The traction tests were performed by setting the following parameters: pre-fixed distance between clips, ±14.5 mm; traction speed, 25 mm/min<sup>-1</sup> (longitudinal), 5 daN top head. Applied Force and movement (sample stretching and elongation) were recorded and digitalized by PowerLab® 4/35 and by LabChart® Pro software, respectively. Strength and elongation were continuously registered till sample breakage. Before the traction tests, width and length of specimens were measured by a caliper while their thicknesses were measured by a digital micrometer (Mitutoyo Corporation, Japan). These values were used to obtain the cross-section area, a necessary value required for the calculation of applied stress after dynamometric measurements (stress  $\sigma$  = applied Force/cross section Area). Finally, stress/strain curves were drawn; only linear portion of tendencies (elastic behavior portion) was taken into consideration and their slope, corresponding to the elastic modulus, calculated.

#### 2.6. Attenuated total reflectance Fourier transform infra-red (ATR FT-IR) analysis

FTIR spectra were obtained in the attenuated total reflection mode (ATR), using a Perkin-Elmer spectrometer (Norwalk, CT, USA) equipped with universal-ATR accessory, fitted with a diamond optical element and ZnSe focusing elements. The apparatus operates with a single reflection at an incident angle of 45°. The analysis was carried out on Films at room temperature and ambient humidity. For each spectrum, 32 scans were acquired between 4000 and 650 cm<sup>-1</sup> with a spectral resolution of 2 cm<sup>-1</sup>.

#### 2.7. Differential scanning calorimetry (DSC) and Thermogravimetric analysis (TGA)

Thermal properties of films were investigated by using a TA DSC-Q2000 differential scanning calorimeter, equipped with a TA Instruments DSC cooling system. Dry nitrogen gas with a flow rate of 20 ml/min was purged through the cell during the measurements and

the thermal treatments. Samples of approximately 5 mg were heated from 20 to 200 °C and kept at this temperature for 2 min, then cooled from 200 to 25 °C, kept at this temperature for 2 min and re-heated from 25 to 200 °C. Heating/cooling rate was fixed to 20 °C/min in all the experiments. To determine the glass transition temperature of alginate the following thermal procedure was applied: samples were heated from 20 to 130 °C at 20 °C/min, kept at this temperature for 1 h, cooled to 20 °C, and re-heated to 200 °C at 20 °C/min.

The thermogravimetric analysis (TGA) analysis has been widely used to study the thermal stability and thermal decomposition of polymers with increasing temperature. The TGA was carried out using a Perkin-Elmer Pyris Diamond TG-DTA apparatus in a nitrogen atmosphere to prevent thermal oxidation. Samples of about 5 mg were heated from 20 to 600 °C at 10 °C/min with a nominal gas flow of 30 ml/min.

#### 2.8. Swelling study

The swelling degree was monitored by measuring water uptake as a function of time. The initial weight of each sample was accurately recorded using an analytical scale, and then they were placed in 5 ml of water in a thermostatic bath at 37 °C. Samples were taken out, excess water was carefully removed using tissue paper, and after being weighed were re-immersed in water. The sample weight was recorded at intervals of 15 min up to 1 h and then after 2, 4, 6 and 24 h (until equilibrium was established). Water was replaced after every weight measurement. The percentage swelling ratio (SR%) at each time point was calculated using Eq. (1):

$$SR\% = \frac{W - W_0}{W_0} \times 100 \quad (1)$$

where  $W$  is the mass of the swollen sample and  $W_0$  is the mass of the initial dry sample.

Assuming that the network swells uniformly in all directions, the equilibrium water content (EWC) can be defined as the ratio between the weight of the swollen sample after 24 h in water and its initial

weight. The equilibrium water content (EWC) percent was calculated by Eq. (2):

$$\text{EWC (\%)} = \frac{W_e - W_d}{W_e} \times 100 \quad (2)$$

where  $W_e$  is the mass of the swollen sample at equilibrium and  $W_d$  is the mass of the dry sample at equilibrium.

### 2.9. Film stability

The stability of ALCur, HALCur 1 and HALCur 2 films was evaluated by placing them in phosphate buffer saline (PBS, NaCl 120 mM, KCl 2.7 mM,  $\text{Na}_2\text{HPO}_4$  10 mM) at pH 7.4, and monitoring weight change with time. Weighed samples were soaked in PBS at 37 °C up to 14 days. At predetermined time intervals (0.5, 1, 6 and 14 days), films ( $n = 4$ ) were removed from phosphate buffer, gently washed with ultrapure water to eliminate any soluble residue, and dried overnight in an oven at 37 °C. The weight loss (%) was calculated as the difference between the initial dry weight of the films ( $W$ ) and the dry weight after incubation ( $W_0$ ) according to the Eq. (3).

$$\text{Weight loss (\%)} = \frac{W - W_0}{W_0} \times 100 \quad (3)$$

### 2.10. Study of curcumin release

The study of curcumin release from ALCur, HALCur 1 and HALCur 2 films was carried out by soaking the films in 10 ml of PBS (pH 7.4) modified with Tween 80 (10% v/v). Tween 80 increases the solubility of curcumin in PBS, preventing the saturation of the release media, and reasonably simulates the *in vivo* conditions in which films could be applied. The Samples were kept under constant stirring at 40 rpm in a water bath shaker at 37 °C. During the release test period (0–10 days), at scheduled times, 1 ml of release medium was withdrawn, and replaced with the same volume of fresh medium. The concentration of released curcumin was determined using a UV-vis spectrophotometer (Synergy H1, BioTek, Winooski, VT), by measuring the absorbance at 426 nm of collected samples. Experiments were performed in triplicate ( $n = 3$ ) and the mean cumulative percentage drug release was calculated using a standard calibration curve. The linearity of the response was verified over the concentration range 0.22–22 µg/ml ( $r^2 = 0.999$ ).

### 2.11. Biological investigation

#### 2.11.1. In vitro cell culture

Biological investigations on curcumin loaded composite films were performed using human dermal fibroblasts (hDF). hDF coded as C84 were isolated and expanded, starting from an underarm explant from a healthy, normolipaemic 45-years old female, and used at passage 28. hDF were cultured in 75 cm<sup>2</sup> cell culture flask in Dulbecco's Modified Eagle Medium (DMEM) supplemented with 10% Fetal Bovine Serum (FBS), antibiotic solution (streptomycin 100 µg/ml and penicillin 100 U/ml, Sigma Chem. Co) and 2 mM L-glutamine. hDF were incubated at 37 °C in a wet atmosphere with 5% CO<sub>2</sub> and 95% air.

#### 2.11.2. Cytotoxicity assay

Biocompatibility represents the first requirement for a medication intended for direct application on injured skin. Toxicity assays of the three types of films developed were assessed in triplicate by first culturing hDF on them, and then evaluating cell viability over 48 h using resazurin assay. ALCur, HALCur 1 and HALCur 2 films were cut in 5 mm disk and sterilized by immersion in a stock penicillin/streptomycin antibiotic solution ( $1 \times 10^7$  U/l) for 1 h, followed by 2 washes in sterile ultrapure water and subsequently kept under the safety cabinet till

drying. Once dehydrated, scaffolds were placed in a 96 well-plate and seeded with hDF. Cells were harvested from the culture flasks at the confluent state by incubation with trypsin solution for 2 min at 37 °C. Cells were then re-suspended with 10% serum-supplemented DMEM, counted and plated at density of  $3 \times 10^4$  cells/well onto the scaffolds. 100 µl of cells resuspension was placed on each scaffold. The same number of cells incubated in the same condition in absence of films was considered as untreated control. Cell viability was evaluated on the basis of the ability to convert resazurin into its fluorescent derivative resarufin. Briefly, at each time point (24; 48 h), scaffolds were transferred into a clear dark 48-well plate and washed with PBS. 300 µl of resazurin solution (250 µg/ml) in DMEM without phenol red with 10% FBS were then added to each well and incubated overnight at 37 °C in the dark. Fluorescence was recorded at 560 nm excitation and 590 nm emission by a Spark® microplate reader (Tecan, Switzerland). Absorbance obtained from correspondent empty scaffolds was subtracted from each measurement.

### 2.12. Antioxidant activity

Antioxidant scavenging activity of the curcumin loaded films was measured by DPPH test. This colorimetric assay consists of the occurring of the scavenging chemical reaction between a solution of the stable radical 2, 2-diphenyl-1-picrylhydrazyl (DPPH) with the supposed antioxidant compound. The reaction changes the DPPH UV absorption band decreasing its optical absorption at 517 nm when the DPPH molecule is reduced from an antioxidant compound (turning color of the solution from violet to yellow). Briefly, a test solution composed of 8.5 ml of acetonitrile, 1 ml of a stock solution of DPPH 1 mM in ethanol (final concentration 100 mM), and 0.5 ml of deionized water was prepared before the experiment. The test specimens (disks with diameter 1.5 cm) were placed in an amber jar ( $n = 3$ ) together with 10 ml of the test solution and kept under stirring in the dark on an orbital shaker for 60 min at room temperature. A control sample consisting of an amber jar containing 10 ml of test solution was also measured as a control sample. At predetermined time intervals (each 20 min), 1 ml of the sample was collected and the vials were immediately replenished with an equivalent volume of test solution. The absorbance of the collected samples was systematically read through a Perkin Elmer - Lambda 25 spectrophotometer measuring the absorbance at 426 nm. A solution of ethanol/deionized Water (95:5 v/v) was used as blank sample during the measurement. The scavenging percentage at each time point was calculated as Eq. (4).

$$\text{DPPH scavenging effect (\%)} = \frac{A_0 - A}{A_0} \times 100 \quad (4)$$

where  $A_0$  is the absorbance of the control sample and  $A$  is the absorbance in the presence of the sample at any time. Decoloration and subsequent decrease of absorbance at 517 nm indicated proportional antioxidant charge increase of the sample tested.

### 2.13. Statistical analysis

Statistical analyses were undertaken using GraphPad Prism®, version 6.00 (GraphPad Software, La Jolla California USA) using one-way ANOVA test. All experiments were performed in triplicate and the results were expressed as the mean  $\pm$  standard deviation (SD). A  $p$ -values below 0.05 considered as significant.

## 3. Results and discussion

### 3.1. Preparation of composite films

Native body tissues can be viewed as complex materials since they include several extracellular matrix components with different features

and properties. For this reason, a one-component material cannot be used to fully replicate the complex mechanics and the biochemical attributes of tissues. Despite the extensive description of elastin and elastin-like peptides use to prepare cross-linked gels, fibers, or injectable scaffolds for tissue engineering and drug delivery [3,13,15,24] their use in applications such as wound dressing or regenerative medicine has to be further improved. The preparation of a composite material based on the natural polymer alginate loaded with a recombinant form of the Human Elastin-Like Polypeptide (HELP) well described and characterized by our group [25,26] represents a valuable approach to reach this goal.

In our laboratory, synthetic genes based on the repeated hexapeptidic motifs that characterize human tropoelastin have been cloned and the expression products were purified through inverse transition cycling [26]. The recombinant technology used to produce HELPs provides precise control over the structure and properties of the final polypeptide resulting in highly homogeneous derived materials. Moreover, the purification of expressed HELP achieved through the inverse phase transition, allows obtaining a highly purified recombinant polypeptide.

Composite films with (HALCur 1 and HALCur 2) and without (ALCur) HELP were prepared by solvent casting followed by the crosslinking, using a calcium chloride solution (Fig. S1). The physical interactions between alginate chains and calcium ions leads to the formation of a well-defined structure, popularly known as the “egg-box model”, in which  $\text{Ca}^{2+}$  ions are embodied in cavities like eggs in a cardboard egg box [27,28]. The resulting chain-to-chain interactions that are formed with the crosslinking increase the structural cohesion of the alginate-based films, leading to higher values of tensile strength and low solubility in water [29]. The same curcumin loading was employed to assess the effect of HELP on the final composite film properties. Glycerol was added as a plasticizer to all the formulations to increase the handling properties and to facilitate the removal from the Petri dish [30]. After crosslinking, the films were flexible, transparent, and uniform with no evident physical defects. The addition of curcumin conferred a yellowish color to these composite films compared to Ca-ALG films that were transparent. A more accurate examination of the surfaces of the composite films was carried out by SEM imaging. Representative SEM micrographs at the same magnification of the tested specimens are compared in Fig. 2. All films displayed a homogeneous structure without any large cracks, air bubbles or evident sign of phase separations, which indicate a good quality polymeric film. However, in presence of HELP the images shown a heterogeneous surface with small aggregates that seems to be influenced by concentration. In particular, ALCur presents a quite smooth surface, characterized by few imperfections consisting of soft protuberances at the surface. These structures increase in terms of numbers proportionally with HELP's increase, becoming almost fibrillar elements ( $\pm 10 \mu\text{m}$  in length) in the most concentrated sample (Fig. 2C). Different roughness could have an influence on cell behavior in contact with the films tested,

however, the biological investigation did not show significant pieces of evidence of enhancement rather than inhibition of cell viability.

### 3.2. Film characterization

#### 3.2.1. Mechanical properties

The mechanical properties of biomaterials, in particular those designed for tissue applications, need to be carefully characterized to fulfil the requisites for a targeted application. The ability to resist to mechanical stress of a material is a valuable physical property that can affect the material behavior both for the manipulation and for the adaptation to the tissues. With the dispersion of HELP into the alginate matrix, we aimed to increase the flexibility of the composite material to make it suitable in applications as skin substitutes and wound dressings, where a degree of elasticity is essential [31,32]. The elastic deformation of a material is well represented by Young's modulus and by the percent elongation at break ( $\epsilon_{\text{break}}$ ), both reported in Table 1. While the values found for ALCur are in agreement with what reported in literature for a calcium-crosslinked alginate [33], the addition of HELP significantly increases Young's modulus and reduces the  $\epsilon_{\text{break}}$ , resulting in an increase in the hardness with increasing concentration of HELP (Fig. S3). This effect can be attributed to the formation of a closer network in presence of HELP, due to molecular entanglements, as will be described in detail in the next paragraphs. The worsening of the mechanical properties of the composites with increasing concentration of HELP can be attributed to alignment, compatibility and specific interactions of the polypeptide with the alginate chains. Further work is in progress to better investigate this point. However, the maximum applied force (the force applied to the sample at the moment of breaking) doesn't present any significant difference among the specimen tested and can be considered high enough to allow easy manipulation of the films avoiding breakage.

#### 3.2.2. FT-IR

Spectra of HALCur 2 and HELP are compared with a crosslinked ALG film without curcumin (Ca-ALG) in Fig. 3a (spectrum of HALCur 1 is not reported since peaks of HELP were hardly detectable). HELP shows diagnostic bands at  $\sim 3495$  ( $-\text{OH}$  stretching),  $3288$  ( $\text{N}-\text{H}$  stretching),  $3053$  and  $2964$  ( $\text{C}-\text{H}$  stretching),  $1636$  (amide I,  $\text{C}=\text{O}$  stretching),  $1533$  (amide II,  $\text{N}-\text{H}$  bending). In HALCur 2, the amide I band is hidden by the strong band of curcumin at  $1620 \text{ cm}^{-1}$ , whereas a shift of amide II band to a lower frequency ( $1514 \text{ cm}^{-1}$ ) is detected. This shift accounts for the establishment of interactions between the  $\text{N}-\text{H}$  amidic groups of HELP and ALG *via* hydrogen bonds, as described in details below. No appearance of new bands was detected, indicating that no chemical reaction occurs. From the analysis of the FT-IR spectra obtained from sodium alginate (Na-ALG) and the corresponding crosslinked film (Ca-ALG) (Supplementary material S2), we found that when crosslinked with calcium ions, the ALG bands of carboxylate respectively moved from  $1593$  to  $1587 \text{ cm}^{-1}$  and from  $1403$  to  $1413 \text{ cm}^{-1}$  (Fig. S2). This

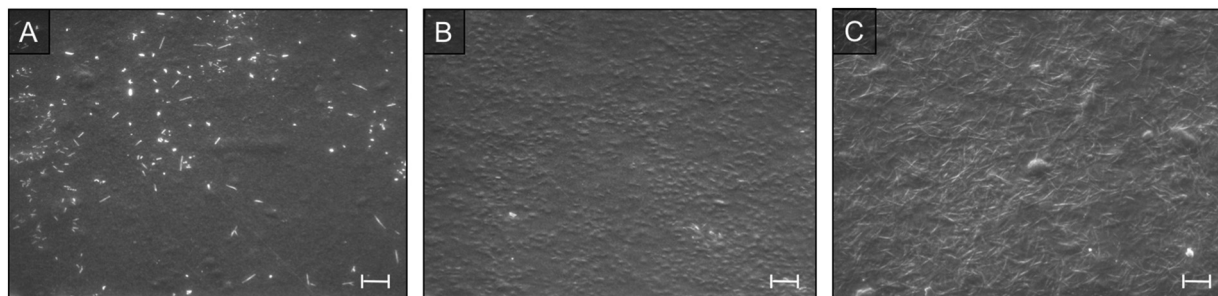


**Fig. 2.** SEM micrograph showing the surface topography of ALG/HELP films. A characteristic highly-corrugated surface structure with small and big wrinkles is formed with increasing HELP concentration. A) ALCur; B) HALCur 1; C) HALCur 2 (magnification 320 $\times$ ; scale bar = 20  $\mu\text{m}$ ).

**Table 1**Thickness, Young modulus (E), elongation at break ( $\epsilon_{\text{break}}$ ) and max applied force  $\pm$  S.D. of films loaded with 0.1% curcumin.

Sample	Thickness ( $\mu\text{m}$ )	E (MPa)	$\epsilon_{\text{break}}$ (%)	Max Applied Force (N)
ALCur	$5.7 \pm 0.9$	$2398 \pm 32$	$1.70 \pm 0.34$	$10 \pm 1$
HALCur 1	$5 \pm 0.6$	$4074 \pm 1249$	$1.10 \pm 0.12$	$10 \pm 1$
HALCur 2	$5.9 \pm 1.3$	$5077 \pm 845$	$0.80 \pm 0.01$	$10 \pm 1$

shift at higher frequency of the symmetric band is a well know indication of  $\text{Na}^+/\text{Ca}^{2+}$  exchange [34]. In the spectrum of HALCur 2 specimen both the asymmetric and symmetric C=O stretching peaks of ALG carboxylate shift towards higher frequencies ( $1594$  and  $1427$   $\text{cm}^{-1}$  respectively) compared to Ca-ALG. This suggests the establishment of interactions between HELP and carboxylate, that might have an impact

on coordination bond between  $\text{Ca}^{2+}$  and ALG, affecting crosslinking; in fact, the frequency separation between C=O asymmetric and symmetric stretches ( $\Delta\nu_{\text{a-s}}$ ), decreases to  $164$   $\text{cm}^{-1}$ , which is somewhat lower than in the case of Ca-ALG (Supplementary material S2).  $\Delta\nu_{\text{a-s}}$  values well below  $200$   $\text{cm}^{-1}$  are compatible with the so-called bidentate “pseudo-bridging” coordination arrangement, in which one of the two

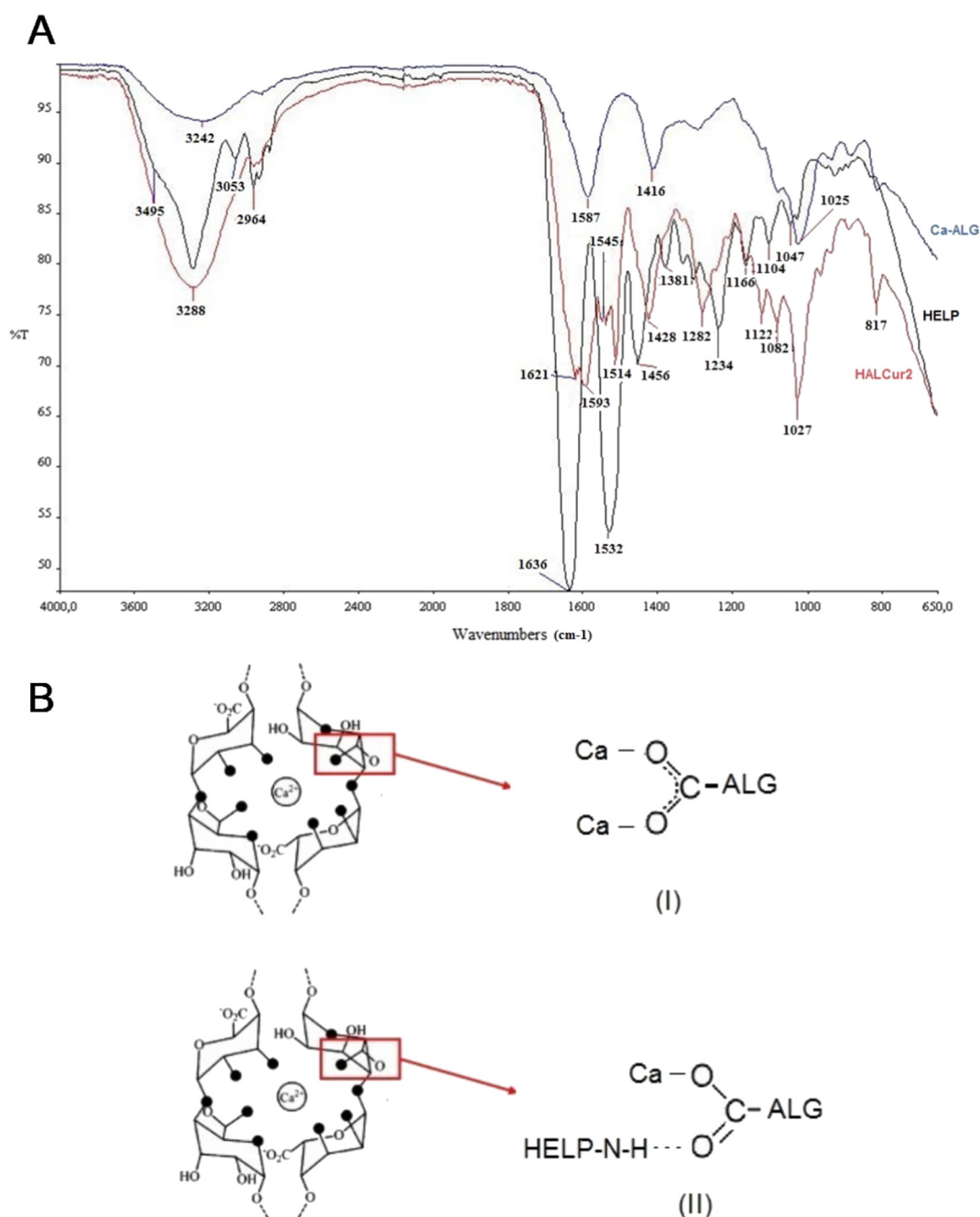


**Fig. 3.** A) FTIR spectra of HALCur 2, HELP and Ca-ALG. B) Egg-box structure of calcium alginate with the two different calcium-carboxylate coordination types: (I) bidentate bridging coordination (Ca-ALG); (II) bidentate pseudo-bridging coordination (HALCur 2).

oxygen atoms is hydrogen bonded to water or another ligand. Therefore, formation of hydrogen bonds between carboxylate and N—H of amidic groups of HELP can be envisaged, as proposed in Fig. 3b.

According to literature [35], FTIR spectrum of pure curcumin have a series of major peaks at 3508  $\text{cm}^{-1}$  (free O—H stretching of phenol group),  $\sim 3300 \text{ cm}^{-1}$  (-OH stretching), 1620  $\text{cm}^{-1}$  (mixed C=O and C=C stretching), 1601  $\text{cm}^{-1}$  (aromatic —C=C— stretching), 1505  $\text{cm}^{-1}$  (C=O stretching) and 1270  $\text{cm}^{-1}$  (enol C—O stretching). Furthermore, the peaks at 713, 856, 886 and 961  $\text{cm}^{-1}$  indicate the bending vibrations of C—C—H and C—H bond of aromatic ring (Fig. S3, Supplementary material). Peaks of curcumin and ALG are retained at the same frequency in ALCur (not shown), indicating the absence of interactions with ALG, whereas a shift of the C—O band of curcumin to 1282  $\text{cm}^{-1}$  was found in HALCur 2. This can be considered an evidence of complex formation, likely involving hydrophobic sequences of HELP.

### 3.2.3. Differential scanning calorimetry (DSC) and thermogravimetric analysis (TGA)

The thermal behavior of the curcumin-loaded films was analyzed by DSC. Raw ALG thermogram exhibited an exothermic peak at 242 °C, resulting from polymer degradation. In the thermogram of all cross-linked samples, this peak disappeared due to the formation of an “egg-box” structure around calcium ions, which increases the degradation temperature of ALG [36]. The thermogram of curcumin showed a very sharp endothermic peak at 182 °C with an associated melting enthalpy of 137,6 J/g. In ALCur, the peak was still present, but shifted to a lower temperature and appeared broadened (168,9 °C, 130,8 J/g). The dispersion within the alginate matrix limits the capability of curcumin to crystallize, as demonstrated by the decrease of melting temperature. In the presence of HELP, the melting endotherm completely disappeared in both HALCur 1 and HALCur 2 thermograms. These results suggest the occurrence of interactions with HELP that prevent the crystallization of curcumin.

The glass transition temperature ( $T_g$ ) of ALG in crosslinked samples was determined during the second run after complete removal of water.  $T_g$  of raw ALG was not reported because not reliably detectable. The complete results are reported in Table 2. The addition of HELP to film formulation causes an increase of alginate  $T_g$ , likely due to interactions of the polypeptide with carboxylate group, as previously described in the FT-IR analysis paragraph, thus confirming that presence of HELP can modify the crosslinking strength and density.  $T_g$  increases proportionally to the HELP content, as expected.

To further explore the interaction between HELP and the crosslinked alginate matrix, the composite films were characterized by TGA from 20 to 600 °C, recording the weight loss as a function of temperatures. Thermogravimetric analysis was performed to study polymer degradation, which is influenced by physical interactions between the components and to evaluate the water content of different samples. Table 2 lists the weight loss up to 150 °C, the onset temperature ( $T_{\text{onset}}$ ) of the whole degradation process, and the temperature of the maximum degradation rate, which corresponds to peaks in the derivative plot ( $T_{\text{peak}}$ ).

**Table 2**

Thermal characteristics of the raw materials used to prepare the composite films, of the crosslinked alginate film without curcumin (Ca-ALG), and of the ALCur, HALCur 1, and HALCur 2 films loaded with 0.1% curcumin. The average relative error on DSC and TGA data is lower than 10%.

	$T_g$	WL (%) up to 150 °C	$T_{\text{onset}}$ (°C)	$T_{\text{peak 1}}$ (°C)	$T_{\text{peak 2}}$ (°C)
HELP	–	8.7	208	328	
Curcumin	–	–	204	362	
ALG	n.d.	16.9	246	268	
Ca-ALG	104	20.4	211	232	256
ALCur	98	17.3	208	229	274
HALCur 1	109.	15.5	210	226	278
HALCur 2	111	16.0	212	225	295

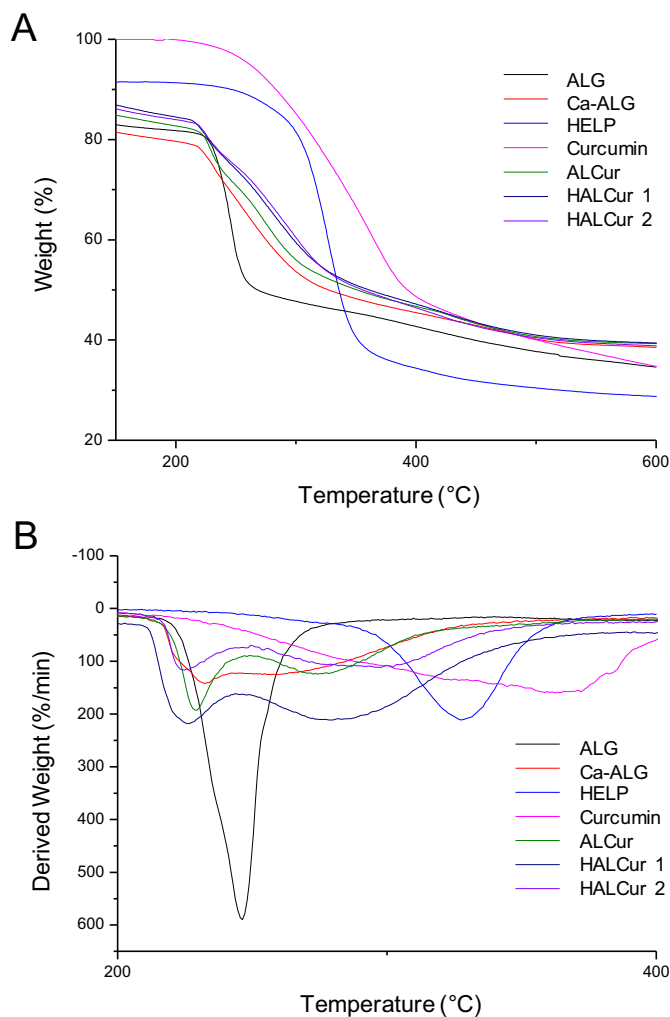


**Fig. 4.** TGA (A) and DTG (B) curves of raw materials (ALG, HELP, and curcumin), crosslinked alginate film without curcumin (Ca-ALG), and ALCur, HALCur 1, and HALCur 2 films loaded with 0.1% curcumin.

Fig. 4a and b shows the weight loss curve and its derivative (DTG) as a function of temperature, respectively. The HELP thermogram shows a sharp degradation from 190 to 400 °C, with a maximum weight loss at 327 °C (12.28%/min), while degradation of curcumin occurs between 175 and 545 °C with a maximum weight loss at 362 °C (4.72%/min). The raw alginate and all the crosslinked samples (ALCur, HALCur 1 and HALCur 2), thermograms show two different weight loss events. The first weight loss (around 15%) up to 150 °C corresponds to the evaporation of water [37]. The second stage above 200 °C is related to degradation phenomena. The derivative thermogravimetry (DTG) curves show the thermal events in the region where degradation occurs (Fig. 4b). DTG curve of ALG shows a single peak with a maximum at around 246 °C (15.82% /min), related to thermal degradation of both mannuronic and guluronic units. In the case of Ca-ALG, two partially overlapping events can be distinguished, suggesting that two structures with different degradation profiles coexist. These different phenomena are related to mannurate and guluronate segments (peak1 and peak2, respectively) [38,39], which are differently involved into the polymer three-dimensional network. In particular, mannuronic moieties, which are not involved in crosslinking, undergo an early degradation ( $T_{\text{peak 1}}$  232 °C), whereas guluronic units degrade at a higher temperature ( $T_{\text{peak 2}}$  259 °C) since they tightly interact with calcium ions in the egg-box structure.

In the thermograms of HALCur samples, a single-step degradation curve, mainly attributed to ALG, is detected. This evidence is consistent with physical interactions, *via* hydrogen bonds, between HELP and ALG chains. Moreover, the addition of HELP to film formulation results in an increase of guluronic moieties degradation temperature. This result suggests that HELP interacts preferentially with guluronic units, and is entangled in the three-dimensional polymer network. In the case of HALCur 2, degradation temperature of guluronate segments increases of around 20 °C with respect to Ca-ALG, thus demonstrating that a higher amount of HELP significantly stabilizes alginate crosslinks.

### 3.2.4. Swelling, equilibrium water content and stability

The ability of a material to absorb water depends on its physical structure and it is related to specific material properties as a uniform and prolonged release of the drug and bioadhesion potential [40]. Swelling of HAL films in PBS was investigated in water and the differences in swelling capacity depending on the amount of HELP content are shown in Fig. 5A. The water uptake of the composite films was rapid and reached its maximum 1 h after contact with water. The curves show that after 1 h the maximum swelling was achieved for all the formulations ( $81.0\% \pm 4.2$ ,  $90.0\% \pm 3.8$ ,  $90.4\% \pm 3.5$  for ALCur, HALCur 1, HALCur 2 respectively) with a significantly ( $p < 0.05$ ) higher percentage swelling for the HALCur 1 and HALCur 2 films. No significant differences in the swelling ratio were found between HALCur 1 and HALCur 2 throughout the experiment. The swelling behavior was followed for 24 h and a slight swelling decrease percentage, probably due to a material loss, was observed. However, after 24 h significant differences are still found in swelling between the samples. HELP affects also the total amount of water that these systems can absorb. The EWC of HALCur 1 and HALCur 2 are  $43.6\% \pm 0.8$  and  $45.5\% \pm 1.8$  respectively, significantly higher if compared with the  $40.9\% \pm 2.2$  recorded for the ALCur film.

The stability profiles of the HAL films in physiological conditions were investigated, monitoring weight changes with time. At each time point, HALCur 1 and HALCur 2 films showed higher degradation than the ALCur. After 7 days of incubation, the films containing HELP appeared more fragile and at 12–14 days of incubation no insoluble material could be detected after visual inspection (Fig. 5B). In our hypothesis, this degradation behavior may further confirm the interactions between the HELP and the carboxylate group of alginate previously detected by FT-IR, DSC, and TGA. In HALCur 1 and HALCur 2 a weight loss of about 30% is already evident after 12 h and it could

be attributed to the easy solubilization in the aqueous release media of the HELP fraction, with the consequent weakening of the entire film structure.

### 3.3. Curcumin release

The release profile of curcumin from HAL composite films was assessed in PBS at pH 7.4 and 37 °C, simulating physiological conditions. Curcumin in the loaded films showed controlled release profiles with a limited initial burst (Fig. 6). After 10 days, over 60% of the total curcumin contained in the films was released with significant differences in the release rate depending on the formulation tested. These differences are more evident during the first 8 h, where the release rate steadily increases to reach a total percent release of  $15.46 \pm 2.45$ ,  $21.28 \pm 1.93$ ,  $29.40 \pm 3.23$  for ALCur, HALCur 1, and HALCur 2 respectively (Fig. 6, inset). The release experiments were conducted up to 10 days to carefully assess both short and long-term release dynamics, as well as the capability of the films to retain the curcumin. Even for a longer period, the amount of curcumin released into the soaking medium is higher in the presence of HELP, with a rising trend correlated to the total HELP amounts. The drug release from the swellable scaffolds mainly depends on water uptake kinetics, pointing to the presence of HELP as a key parameter in affecting the release rate. As previously discussed, films containing HELP have higher water uptake, a feature that appears to be related to the release profile as well. The presence of HELP into an alginate matrix or film can therefore also be used to control the release of a hydrophobic drug, modifying the structural features of the matrix and tuning the release of the loaded drug.

### 3.4. Cytotoxicity assay

Biological studies were conducted to demonstrate if the developed composites, differing each other for HELP content (0 to 0.25%), did not show toxic effects on human dermal cells. The second aim of this study consisted in the evaluation of cell proliferation induction due to the presence of HELP in the composites. The *in vitro* cytotoxicity evaluation is a fast method to provide predictive evidence of material biocompatibility. Cytotoxicity of ALG/HELP composites was evaluated on human dermal fibroblasts (hDF), which play an important role in generating connective tissue and allowing the skin to recover from injury [41]. Fig. 7 shows the effect of the films on the viability of hDF assessed

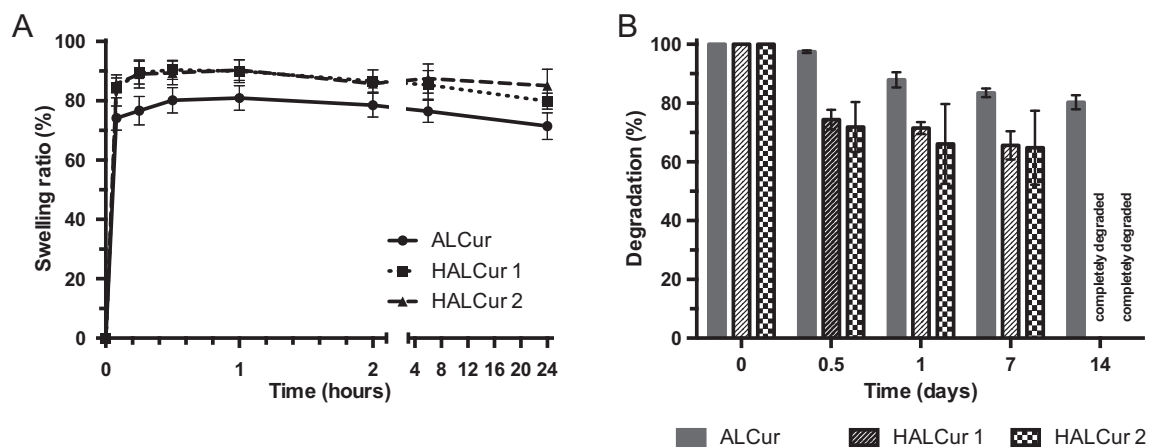


**Fig. 5.** Swelling (A) and stability (B) profiles of ALCur, HALCur 1, and HALCur 2 films loaded with 0.1% curcumin ( $n = 3, \pm SD$ ). After 24 h HALCur 1, and HALCur 2 films have a significantly ( $p < 0.05$ ) higher swelling capacity vs ALCur, while the difference between HALCur 1, and HALCur 2 was not significant. Similarly, the stability is related to the HELP presence, with the HALCur 1, and HALCur 2 films more susceptible to degradation after 14 days of immersion in PBS at 37 °C.

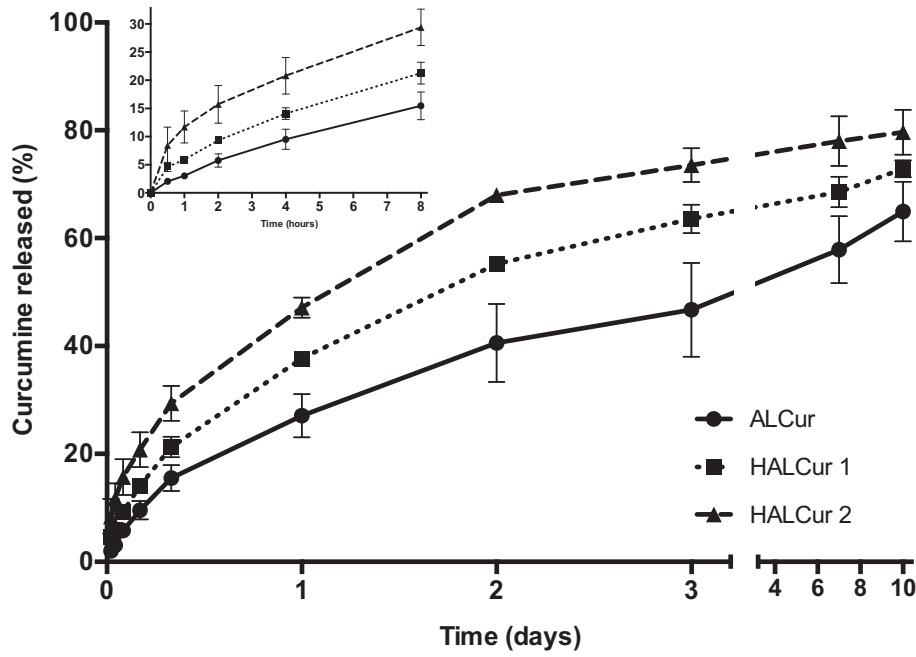


**Fig. 6.** Cumulative curcumin release (%) profiles from ALCur, HALCur 1, and HALCur 2 films. Results are reported as mean  $\pm$  standard deviation of three independent measurements. Lines through data points are to guide the eye.

by resazurin assay. After 24 h of incubation, the ALCur replicas showed the lowest cell viability ( $63\% \pm 9$ ), comparing it with the control group. HALCur 1 and HALCur 2 showed a viability of  $80\% \pm 1$  and  $72\% \pm 4$ , respectively. The evaluation at 48 h, ALCur had the lower viability of  $60\% \pm 4$ , HALCur 1 scored  $73\% \pm 8$  and HALCur 2,  $72\% \pm 5$ . At both these time points, the cell viability of ALCur is still around 60% while for HALCur 1 and HALCur 2 viability is significantly higher. According to the recommended guidelines for the evaluation of *in vitro* cytotoxicity for medical devices and delivery systems (DIN EN ISO 10993-5), a biomaterial can be deemed non-cytotoxic if the cell viability after exposure does not fall below the 70% [42]. The ALCur films resulted in the lowest

values in terms of viability respect the controls, Conversely, in the presence of HELP in all cases the cell viability is higher of 70% both at 24 and 48 h. These data suggest a cell proliferation enhancement effect of HELP on hDF, and this is consistent with the previous observation that elastin-like polypeptides may exert a pro-proliferative effect [43]. Therefore, the results obtained in the present study show that the HAL composite films loaded with curcumin could be considered as potentially biocompatible and generally safe.

### 3.5. Antioxidant activity

It is well known that chronic skin wound oxidation represents a major etiological cause of macromolecular damages during the tissue

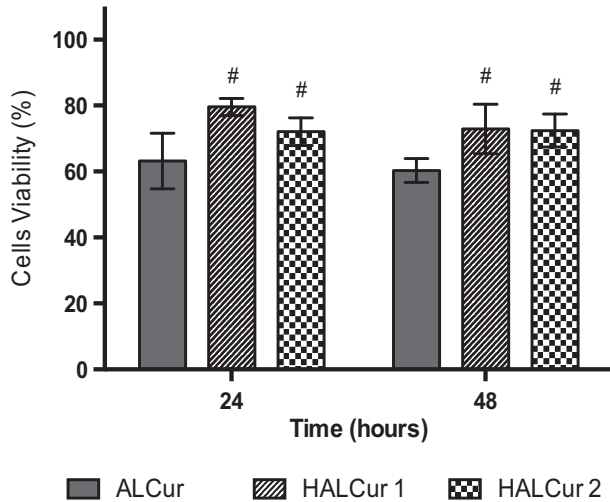


**Fig. 7.** Effect of ALG/HELP composite biomaterials on human dermal fibroblasts cells viability. Cell viability has been determined by resazurin assay. The results have been reported as percentage of viable cells compared with the control considered as 100% viable cells. Bars represent the mean  $\pm$  SD of triplicate determination in 3 independent experiments. # $p < 0.05$  vs. ALCur.

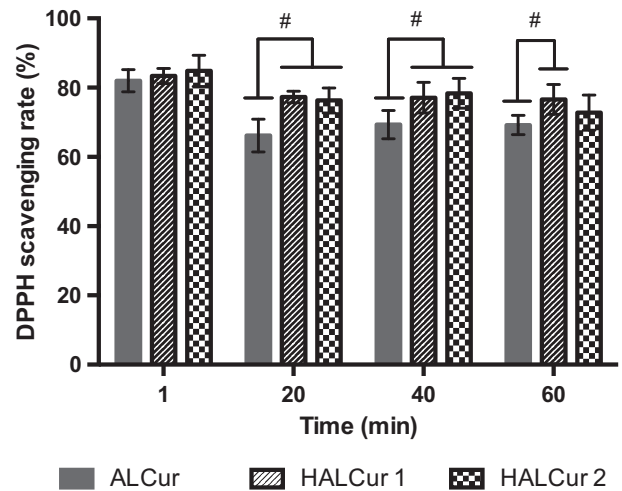


**Fig. 8.** *In vitro* antioxidant activity of the ALCur and HALCur films measured by the DPPH assay. Bars represent the mean  $\pm$  SD of triplicate determination in 3 independent experiments. # $p < 0.05$ .

regeneration process. ECM proteins, in particular, can be damaged by Reactive Oxygen Species (ROS) activity due to their high chemical reactivity and capability to oxidize cellular macromolecules [44]. ROS are produced in significant amounts from macrophages invading the wound area during inflammation, playing a crucial role as signalling molecules as well as antimicrobial compounds [45]. However, the prolonged tissue exposition to high concentrations of oxidative stress gives a significant contribution both to the insurgence and persistence of chronic wounds and other pathologies. The natural phenolic compound Curcumin has well demonstrated antioxidant and anti-inflammatory effects by carrying out scavenging activity of free radicals, lowering lipid peroxides [46–48]. These inherent properties make curcumin particularly suitable for the treatment of various damaged tissues, as wound injuries. In particular, its antioxidant and radical scavenging activity can be exploited to control wound oxidative stress and thereby accelerate wound healing [46,49]. Animal studies suggest that supplementation of this compound could enhance/ameliorate the tissue repair process [50]. In this work, we performed an antioxidant scavenging activity assay to verify if the antioxidant activity of curcumin is maintained even after dispersion in ALG/HELP films. The results (Fig. 8), confirmed the strong *in vitro* antioxidant activity of the developed alginate-based composites containing curcumin 0.1% w/w. As expected, no significant differences were detected among the sampling time points. In particular, in all the samples tested the scavenging activity on DPPH molecule ranged from  $66.2 \pm 4.7\%$  to  $84.9 \pm 4.5\%$ . Interestingly, the difference in the antioxidant activity observed among the samples that were analyzed at later time points appeared related to the presence of HELP in the composite. This suggests that the HELP component favours the release of the curcumin although further studies are needed to support these results. In conclusion, the composites resulted effective as free radical scavengers showing the potential application in medical devices that can improve the wound healing process and proper skin regeneration.

#### 4. Conclusion

This study aimed to test the properties of a series of composite films based on the natural polymer alginate and a recombinant form of human elastin that can be loaded with bioactive components. There are only a few examples of elastin-like based composites that have been developed till now, and with this work, we have demonstrated how the combination of alginate and HELP allowed tuning the final properties of the resulting material, thus modulating the delivery of curcumin, a natural molecule used as a model antioxidant compound. Our study showed that the fabrication of the composite is feasible and that the features of the two components can be successfully integrated. Stable films based on alginate and HELP were easily prepared establishing a protocol. FT-IR and thermal analysis evidenced an interaction between HELP and the carboxylate group of alginate, a phenomenon that is likely correlated to the final functional features of the material. The presence of HELP in the composite was shown functional both to control the release of the model compound curcumin leading to a high antioxidant activity of the material and to maintain, and possibly enhance, the cytocompatibility of the final material. Overall, although further studies are needed to evaluate the *in vivo* behavior of this composite material, our work demonstrated that the association of alginate with HELP was effective to prepare customizable platforms for drug delivery, wound healing, and tissue regeneration. Finally, it worth noticing that HELP-based proteins are readily customizable by molecular fusion of exogenous domains to prepare active biopolymers. These HELP fusion proteins may represent in the future a further possibility to confer specific functionality to the final composite materials.

#### Author statement

**Carlo Bergonzi:** Investigation, Visualization, Data curation, Writing - Original draft preparation; **Giovanna Gomez d'Ayala:** Investigation,

Visualization, Data curation, Writing - Original draft preparation; **Lisa Elviri:** Supervision; **Paola Laurienzo:** Supervision, Methodology, Writing - Review & Editing; **Antonella Bandiera:** Supervision, Funding acquisition; **Ovidio Catanzano:** Investigation, Visualization, Methodology, Data curation, Writing - Review & Editing, Supervision.

#### Declaration of competing interest

The authors declared that there is no conflict of interest.

#### Acknowledgement

This work was funded by "Commissariato del Governo della Regione Friuli Venezia Giulia - Fondo Trieste" and managed by AREA Science park in the frame of "Made in Trieste" program. The authors are very grateful to Dr. Annalisa Bianchera for her precious help during cytotoxicity studies. The authors wish to thank Dr. M. Stebel for technical assistance in HELP polypeptide production and Prof. S. Passamonti for scientific assistance during the project.

#### References

- [1] D. Akilbekova, M. Shaimerdenova, S. Adilov, D. Berillo, Biocompatible scaffolds based on natural polymers for regenerative medicine, *Int. J. Biol. Macromol.* 114 (2018) 324–333.
- [2] A. Bianchera, O. Catanzano, J. Boateng, L. Elviri, The Place of Biomaterials in Wound Healing, *Therapeutic Dressings and Wound Healing Applications*, 2020 337–366.
- [3] E. Salernitano, C. Migliaresi, Composite materials for biomedical applications: a review, *J Appl Biomater Biomech* 1 (1) (2003) 3–18.
- [4] H. Semyari, M. Salehi, F. Taleghani, A. Ehterami, F. Bastami, T. Jalayer, H. Semyari, M. Hamed Nabavi, H. Semyari, Fabrication and characterization of collagen-hydroxyapatite-based composite scaffolds containing doxycycline via freeze-casting method for bone tissue engineering, *J. Biomater. Appl.* 33 (4) (2018) 501–513.
- [5] J. Boateng, R. Burgos-Amador, O. Okeke, H. Pawar, Composite alginate and gelatin based bio-polymeric wafers containing silver sulfadiazine for wound healing, *Int. J. Biol. Macromol.* 79 (2015) 63–71.
- [6] D. Zamani, F. Mozartzadeh, D. Bizari, Alginate-bioactive glass containing Zn and Mg composite scaffolds for bone tissue engineering, *Int. J. Biol. Macromol.* 137 (2019) 1256–1267.
- [7] J. Venkatesan, I. Bhatnagar, P. Manivasagan, K.H. Kang, S.K. Kim, Alginate composites for bone tissue engineering: a review, *Int. J. Biol. Macromol.* 72 (2015) 269–281.
- [8] R. Silva, R. Singh, B. Sarker, D.G. Papageorgiou, J.A. Juhasz-Bortuzzo, J.A. Roether, I. Cicha, J. Kaschta, D.W. Schubert, K. Chrissafis, R. Detsch, A.R. Boccaccini, Hydrogel matrices based on elastin and alginate for tissue engineering applications, *Int. J. Biol. Macromol.* 114 (2018) 614–625.
- [9] J. Halper, M. Kjaer, Basic components of connective tissues and extracellular matrix: elastin, fibrillin, fibulins, fibrinogen, fibronectin, laminin, tenascins and thrombospondins, in: J. Halper (Ed.), *Progress in Heritable Soft Connective Tissue Diseases*, Springer Netherlands, Dordrecht 2014, pp. 31–47.
- [10] F.W. Keeley, C.M. Bellingham, K.A. Woodhouse, Elastin as a self-organizing biomaterial: use of recombinantly expressed human elastin polypeptides as a model for investigations of structure and self-assembly of elastin, *Philos T R Soc B* 357 (1418) (2002) 185–189.
- [11] V. Groult, W. Hornebeck, P. Ferrari, J.M. Tixier, L. Robert, M.P. Jacob, Mechanisms of interaction between human skin fibroblasts and elastin - differences between elastin fibers and derived peptides, *Cell Biochem. Funct.* 9 (3) (1991) 171–182.
- [12] S. Ito, S. Ishimaru, S.E. Wilson, Effect of coacervated alpha-elastin on proliferation of vascular smooth muscle and endothelial cells, *Angiology* 49 (4) (1998) 289–297.
- [13] Q. Wen, S.M. Mithieux, A.S. Weiss, Elastin biomaterials in dermal repair, *Trends Biotechnol.* 38 (3) (2019) 280–291.
- [14] W.F. Daamen, T. Hafmans, J.H. Veerkamp, T.H. van Kuppevelt, Comparison of five procedures for the purification of insoluble elastin, *Biomaterials* 22 (14) (2001) 1997–2005.
- [15] D. Miranda-Nieves, E.L. Chaikof, Collagen and elastin biomaterials for the fabrication of engineered living tissues, *ACS Biomater Sci Eng* 3 (5) (2017) 694–711.
- [16] G. Ciofani, G.G. Genchi, V. Mattoli, B. Mazzolai, A. Bandiera, The potential of recombinant human elastin-like polypeptides for drug delivery, *Expert Opin Drug Deliv* 11 (10) (2014) 1507–1512.
- [17] G. Ciofani, G.G. Genchi, P. Guardia, B. Mazzolai, V. Mattoli, A. Bandiera, Recombinant human elastin-like magnetic microparticles for drug delivery and targeting, *Macromol. Biosci.* 14 (5) (2014) 632–642.

- [18] A. Bandiera, Transglutaminase-catalyzed preparation of human elastin-like polypeptide-based three-dimensional matrices for cell encapsulation, *Enzyme Microb Tech* 49 (4) (2011) 347–352.
- [19] P. D'Andrea, D. Civita, M. Cok, L.U. Severino, F. Vita, D. Scaini, L. Casalis, P. Lorenzon, I. Donati, A. Bandiera, Myoblast adhesion, proliferation and differentiation on human elastin-like polypeptide (HELP) hydrogels, *J Appl Biomater Func* 15 (1) (2017).
- [20] P. D'Andrea, M. Sciancalepore, K. Veltruska, P. Lorenzon, A. Bandiera, Epidermal growth factor - based adhesion substrates elicit myoblast scattering, proliferation, differentiation and promote satellite cell myogenic activation, *Bba-Mol Cell Res* 1866 (3) (2019) 504–517.
- [21] L. Corich, M. Buseti, V. Petix, S. Passamonti, A. Bandiera, Evaluation of a biomimetic 3D substrate based on the Human Elastin-like Polypeptides (HELPS) model system for elastolytic activity detection, *J. Biotechnol.* 255 (2017) 57–65.
- [22] A. Bandiera, A. Markulin, L. Corich, F. Vita, V. Borelli, Stimuli-induced release of compounds from elastin biomimetic matrix, *Biomacromolecules* 15 (1) (2014) 416–422.
- [23] A. Bandiera, S. Passamonti, L.S. Dolci, M.L. Focarete, Composite of elastin-based matrix and electrospun poly(L-lactic acid) fibers: a potential smart drug delivery system, *Front Bioeng Biotech* 6 (2018).
- [24] A. Bandiera, Elastin-like polypeptides: the power of design for smart cell encapsulation, *Expert Opin Drug Deliv* 14 (1) (2017) 37–48.
- [25] A. Bandiera, Assembly and optimization of expression of synthetic genes derived from the human elastin repeated motif, *Prep Biochem Biotech* 40 (3) (2010) 198–212.
- [26] A. Bandiera, P. Sist, R. Urbani, Comparison of thermal behavior of two recombinantly expressed human elastin-like polypeptides for cell culture applications, *Biomacromolecules* 11 (12) (2010) 3256–3265.
- [27] E.R. Morris, D.A. Rees, D. Thom, J. Boyd, Chiroptical and stoichiometric evidence of a specific, primary dimerisation process in alginate gelation, *Carbohydr. Res.* 66 (1) (1978) 145–154.
- [28] G.T. Grant, E.R. Morris, D.A. Rees, P.J.C. Smith, D. Thom, Biological interactions between polysaccharides and divalent cations: the egg-box model, *FEBS Lett.* 32 (1) (1973) 195–198.
- [29] R. Russo, M. Malinconico, G. Santagata, Effect of cross-linking with calcium ions on the physical properties of alginate films, *Biomacromolecules* 8 (10) (2007) 3193–3197.
- [30] J.S. Boateng, H.N. Stevens, G.M. Eccleston, A.D. Auffret, M.J. Humphrey, K.H. Matthews, Development and mechanical characterization of solvent-cast polymeric films as potential drug delivery systems to mucosal surfaces, *Drug Dev. Ind. Pharm.* 35 (8) (2009) 986–996.
- [31] J. Boateng, O. Catanzano, Advanced therapeutic dressings for effective wound healing—a review, *J. Pharm. Sci.* 104 (11) (2015) 3653–3680.
- [32] J.S. Boateng, K.H. Matthews, H.N. Stevens, G.M. Eccleston, Wound healing dressings and drug delivery systems: a review, *J. Pharm. Sci.* 97 (8) (2008) 2892–2923.
- [33] R. Russo, M. Abbate, M. Malinconico, G. Santagata, Effect of polyglycerol and the crosslinking on the physical properties of a blend alginate-hydroxyethylcellulose, *Carbohydr. Polym.* 82 (4) (2010) 1061–1067.
- [34] G.B. Deacon, R.J. Phillips, Relationships between the carbon-oxygen stretching frequencies of carboxylate complexes and the type of carboxylate coordination, *Coord. Chem. Rev.* 33 (3) (1980) 227–250.
- [35] P.R.K. Mohan, G. Sreelakshmi, C.V. Muraleedharan, R. Joseph, Water soluble complexes of curcumin with cyclodextrins: characterization by FT-Raman spectroscopy, *Vib. Spectrosc.* 62 (2012) 77–84.
- [36] T.S. Pathak, J.S. Kim, S.-J. Lee, D.-J. Baek, K.-J. Paeng, Preparation of alginate and metal alginate from algae and their comparative study, *J. Polym. Environ.* 16 (3) (2008) 198–204.
- [37] M. Rezvanian, N. Ahmad, M.C.I. Mohd Amin, S.-F. Ng, Optimization, characterization, and in vitro assessment of alginate-pectin ionic cross-linked hydrogel film for wound dressing applications, *Int. J. Biol. Macromol.* 97 (2017) 131–140.
- [38] A. Nešić, A. Onjia, S. Davidović, S. Dimitrijević, M.E. Errico, G. Santagata, M. Malinconico, Design of pectin-sodium alginate based films for potential healthcare application: study of chemico-physical interactions between the components of films and assessment of their antimicrobial activity, *Carbohydr. Polym.* 157 (2017) 981–990.
- [39] M.R. Nobile, V. Pirozzi, E. Somma, G. Gomez D'Ayala, P. Laurienzo, Development and rheological investigation of novel alginate/N-succinylchitosan hydrogels, *J. Polym. Sci. B Polym. Phys.* 46 (12) (2008) 1167–1182.
- [40] N.A. Peppas, P.A. Buri, Surface, interfacial and molecular aspects of polymer bioadhesion on soft tissues, *J. Control. Release* 2 (1985) 257–275.
- [41] L.E. Tracy, R.A. Minasian, E.J. Caterson, Extracellular matrix and dermal fibroblast function in the healing wound, *Adv Wound Care (New Rochelle)* 5 (3) (2016) 119–136.
- [42] International Standardization Organisation, ISO 10993-5 Biological Evaluation of Medical Devices, Part 5: Tests for Cytotoxicity, in *Vitro Methods*, Geneva, 1992.
- [43] Y. Yuan, P. Koria, Proliferative activity of elastin-like-peptides depends on charge and phase transition, *J. Biomed. Mater. Res. A* 104 (3) (2016) 697–706.
- [44] M. Schafer, S. Werner, Oxidative stress in normal and impaired wound repair, *Pharmacol. Res.* 58 (2) (2008) 165–171.
- [45] B. D'Autreaux, M.B. Toledano, ROS as signalling molecules: mechanisms that generate specificity in ROS homeostasis, *Nat Rev Mol Cell Biol* 8 (10) (2007) 813–824.
- [46] V.P. Menon, A.R. Sudheer, Antioxidant and anti-inflammatory properties of curcumin, in: B.B. Aggarwal, Y.-J. Surh, S. Shishodia (Eds.), *The Molecular Targets and Therapeutic Uses of Curcumin in Health and Disease*, Springer US, Boston, MA 2007, pp. 105–125.
- [47] V.P. Menon, A.R. Sudheer, Antioxidant and anti-inflammatory properties of curcumin, *Adv. Exp. Med. Biol.* 595 (2007) 105–125.
- [48] G.C. Jagetia, G.K. Rajanikant, Curcumin stimulates the antioxidant mechanisms in mouse skin exposed to fractionated gamma-irradiation, *Antioxidants (Basel)* 4 (1) (2015) 25–41.
- [49] S.D. Fitzmaurice, R.K. Sivamani, R.R. Isseroff, Antioxidant therapies for wound healing: a clinical guide to currently commercially available products, *Skin Pharmacol Phys* 24 (3) (2011) 113–126.
- [50] A.M. Rasik, A. Shukla, Antioxidant status in delayed healing type of wounds, *Int. J. Exp. Pathol.* 81 (4) (2000) 257–263.